THE THERMALHYDRAULICS OF CORIUM POOLS UNDERGOING A MISCIBILITY GAP
MODEL DEVELOPMENT AND REACTOR APPLICATIONS

JM Seiler[1], K Froment[1], F Defoort[1], F Fichot[2]

[1] CEA/DTN - Grenoble
[2] IRSN/DRS - Cadarache

Abstract

The paper describes the behaviour of corium undergoing a miscibility gap (UO2, ZrO2, Zr, Stainless Steel) and the consequences on the molten pool thermalhydraulics for In-Vessel Retention. The methodology will be described for calculation of stratification (including the prediction of inverse stratification) and heat transfer. The interface temperatures and heat flux distributions are consistently derived from material and thermalhydraulic constraints.

The model is validated against the results obtained during the MASCA project and the results obtained on SIMECO (RIT).

Reactor applications will be described. The mass of metal that can stratify below the oxidic phase is estimated, as well as the impact on heat flux distribution on the vessel. The minimum mass of molten steel required for keeping the heat flux below CHF is determined.

Context and objectives

In the frame of the analysis of Light Water Reactors (LWRs) severe accidents, the possibility is investigated of molten core (Corium) recovery in a structure like the lower head (In-Vessel Retention) or a dedicated core-catcher. The determination of the heat loads on the structure is a key to the analysis of the coolability of the structure containing the molten masses. The heat loads associated to molten corium pools (with dissipation of residual power) has been discussed extensively in the past in the frame of a large international collaboration [CSNI 1998]. The RASPLAV programme (Münich, 2000) has addressed the behaviour of real corium. It has been demonstrated that material effects have a strong influence on the stratification of corium and, as a consequence, on the power distribution on the surrounding structures. Phase separation due to a miscibility gap participates to these material effects. Such a situation has been previously emphasised (scenario C from [Rempe et al., 1997]), on the basis of previous material investigations [Powers, 1987], [Kim and Olander, 1988], [Parker and Hodge, 1990], [Hayward and George, 1996] and [Gueneau et al., 1998]. The miscibility gap in the U,O,Zr,Fe system has also been investigated by several authors [Hofmann, 1976], [Parker, 1982], [Gueneau, 1999]. More recently it has been observed again in the frame of the MASCA programme [Bechta, 2001] that the addition of steel to U-O-Zr mixtures could result in a density inversion, the molten metal phase stratifying below the molten oxidic phase. However, a model for the description of the physicochemical and thermalhydraulic behaviour of a corium pool undergoing a phase separation due to a miscibility gap was lacking.

The model developed hereafter applies to the liquid material that reaches physicochemical equilibrium between liquid phases, at some moment in the degradation transient. This is, for instance, the case for In-Vessel situations when molten steel from the vessel (or from lower head internals) comes into contact with the molten oxidic corium. This situation may only concern a part of the steel material contained in the lower head. Another part may be separated from the oxidic material by a crust, and may not come to physicochemical equilibrium with the oxidic liquid. The analysis of which part of the materials may be considered to enter the equilibrium is not the subject here and must be treated separately. Physicochemical equilibrium between oxidic and metallic melts is also obtained in core-catchers designs where a volume of (heavier) liquid metal is placed between a protection ceramic and the (lighter) molten oxidic corium.

The basis for this work is the analysis of the non-eutectic material effects that have been performed previously for mixtures presenting standard solidus and liquidus curves [Seiler and Froment, 2001].

Presentation of the model for corium pool with miscibility gap reaching thermochemical equilibrium

Restrictions

In this paper a binary phase diagram will be used for comprehension and purpose of demonstration. For real corium mixtures (U, O, Zr, Fe,…) it is generally not possible to represent the physicochemical behaviour through binary diagrams. Even if some vertical sections are used (for instance UO_2 - (Zr_xFe_y)), the reader must be aware that such vertical sections generally do not contain the tie-lines. The composition of phases in equilibrium for complex systems must be deduced from thermodynamic equilibrium calculations, using a numerical software. This does not introduce a supplementary difficulty since all the necessary information is derived from these calculations (the main problem is the elaboration and validation of thermodynamic databases).

Isothermal system : behaviour of the mixture at thermodynamic equilibrium

Let us consider a binary mixture of two species A and B having the phase diagram presented on figure 1. The behaviour of the mixture will be described, at thermodynamic equilibrium, for compositions varying between C_1 and C_2 (limits ("edges") of the miscibility gap) and for temperatures varying between T_{min} and $T_{max,\,MG}$.

$T_{max,MG}$ (see figure 1) corresponds to the maximum temperature associated with the miscibility gap. Above this temperature, any mixture of A and B will form a single liquid. T_{MG} (see figure 1) corresponds to the transition temperature into the miscibility gap. Note that it is the liquidus temperature. Let C_0 be the variable composition of the mixture of A and B, with $C_1<C_0<C_2$.When $C_1<C_0<C_2$, the mixture may undergo a separation into two non-miscible liquid phases (curves L1 and L2 for $T_{MG}<T<T_{max,MG}(C_0)$). $T_{max,MG}(C_0)$ is defined on figures 1 and 2. It corresponds to the maximum temperature for which the mixture of composition C_0 may undergo a separation into two non-miscible liquids. The separation occurs when the temperature is greater than T_{MG}, which is the transition temperature into the miscibility gap, or liquidus temperature. At a temperature verifying $T_{MG}<T<T_{max,\,MG}(C_0)$, this mixture will separate into two non-miscible liquids of compositions C_{L1} (T) and C_{L2} (T). The relative amounts of these two liquids is a function of the temperature (T) and is given, at thermodynamic equilibrium, by the lever rule: $x_{L2}(T) = \frac{C_0 - C_{L1}(T)}{C_{L2}(T) - C_{L1}(T)} . x_{L2}(T)$ is the relative amount of liquid L2 at temperature (T) (x is expressed in mole fraction or mass fraction depending on the units of the axis A➔B of the phase diagram). Of course, we have: $x_{L1} + x_{L2} = 1$.

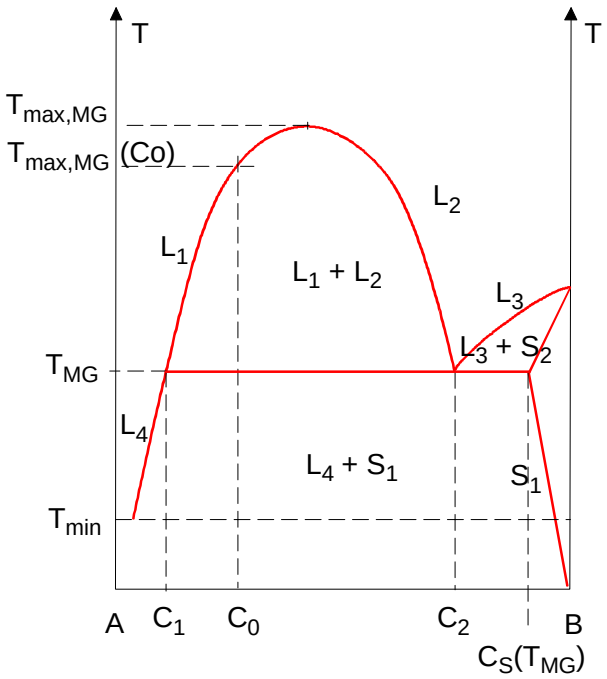

Figure 1: Characteristic binary phase diagram with miscibility gap (MG)

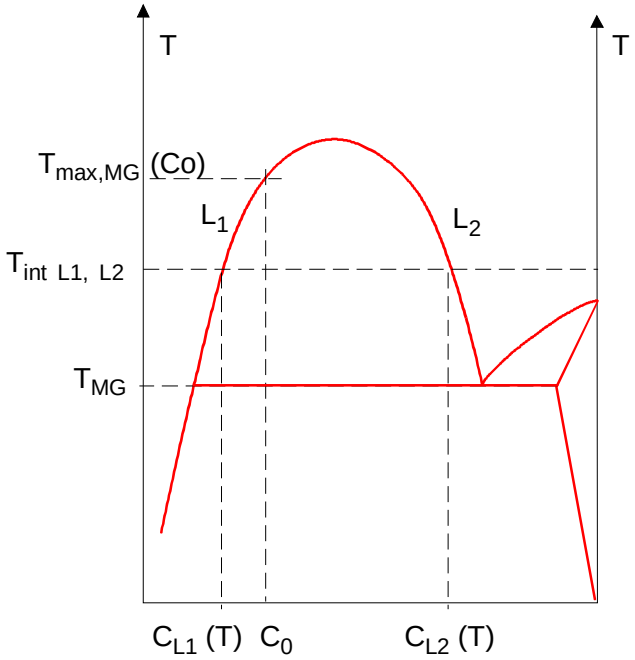

Figure 2: Lever rule in the miscibility gap

When the temperature T increases and tends towards $T_{max, MG}$ (C_0), the liquid L2 disappears and the composition of the liquid L1 tends towards the composition of the mixture (C_0). For T> $T_{max,MG}$(C_0), the single liquid will have the composition C_0.

The densities of the liquids L1 and L2 may be different. Thus, these liquids may undergo gravitational separation (stratification). We will suppose, in the following, that liquid L2 is lighter than liquid L1. When the temperature decreases below T_{MG}, the mixture of composition C_0 undergoes a separation between a liquid phase L4 and the solid S1 (see figure 1). The composition of the liquid L4 and of the solid S1 depends on temperature. The solid phase appears as soon as the decreasing temperature is equal to T_{MG}. At this temperature, the composition of the solid phase is $C_s(T_{MG})$, and the composition of the liquid phase, in equilibrium with the preceding solid is C_1 (see fig 1).

Non isothermal system: analysis of the constraints for a volumetrically heated mixture cooled from the outside

Let us consider the reactor case, i.e., that the preceding mixture is now in a vessel as represented on figure 3. It is further assumed that:

- The mixture is submitted to a volumetric heating; the volumetric heating may be different in the different layers,
- The external temperature (Text) is constant, and low: Text<<T_{MG}),
- The power is high, thus the mixture is mainly liquid,
- The liquid phase L1 is in contact with the liquid phase L2 and come to physicochemical equilibrium,
- A solid crust is deposited at the boundaries. The heat transfer in the solid is controlled by conduction. The thermal conductivity of the solid is supposed to be small, thus the mass fraction of solid is also small (this hypothesis is taken as a first step and could be removed afterwards).

- The system has reached a steady state from the point of view of mass and heat transfer.
- At steady state, the *overall residual (actual) liquid* has composition C_0
- A separation into two liquids is observed for the corresponding steady state (conditions for the existence of this separation will be deduced from the analysis below).

Unlike the cases of usual non-eutectic mixtures considered up to now [Seiler and Froment, 2000], there is not a single interface condition which must be determined here but at least three!

a. the interface condition between the two liquid phases (Int $_{L1,L2}$),
b. the interface condition between liquid L1 and the solid (Int $_{L1, solid}$)
c. and the interface condition between liquid L2 and the solid (Int $_{L2, solid}$) (side and top)

Now, we will analyse, for this system, the physico-chemical aspects and the thermalhydraulic aspects.

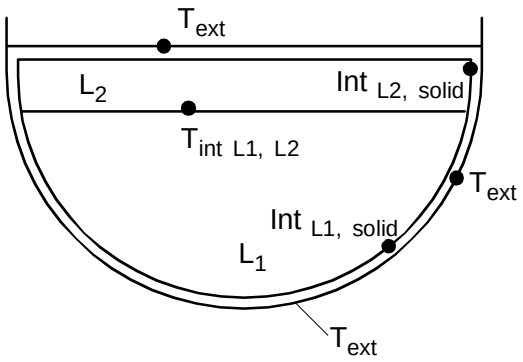

Figure 3 : Lower head geometry - Stratification and interface conditions

The physico-chemical constraints

The physico-chemical constraints need to be determined for the three interfaces previously cited.

Interface L1, L2

Supposing that steady state is reached, the two layers L1 and L2 are established and there is, as a consequence, no net mass transfer between these two layers. This means that the composition of both liquids at the interface is equal to their respective bulk compositions [Seiler and Froment, 2001]. Since thermodynamic equilibrium is established on the interface, this leads to the following straightforward conclusion: both liquids are, in steady state, at thermodynamic equilibrium at the interface temperature between the two liquids. Thus, the lever rule applies to give the relative amount of each liquid:

$$x_{L2}(T_{int\ L1,L2}) = \frac{C_0 - C_{L1}(T_{int\ L1,L2})}{C_{L2}(T_{int\ L1,L2}) - C_{L1}(T_{int\ L1,L2})}$$

("x" is again expressed in mole fraction or mass fraction depending on the units used in the phase diagram). This equation is a link between the interface temperature $T_{int\ L1,L2}$ and the relative amounts (heights) of liquids L1 and L2.

$T_{int\ L1,L2}$ is unknown; and the determination of the relative amount (the height) of both liquids and the interface temperature requires a supplementary equation which will be provided by thermalhydraulic considerations (see § I. 3.2)

The condition for the existence of a separation into two liquid layers can easily be deduced from preceding considerations, and is simply: $T_{MG} < T_{int\ L1,L2} < T_{max,\ MG}(C_0)$

Interface L1-solid and interface L2-solid

At the interface with the solid, the considerations developed for non-eutectic mixtures [Seiler and Froment, 2001] apply and the liquidus temperature is simply replaced by the temperature at which the first solid appears, which is here the transition temperature into the miscibility gap T_{MG} (liquidus temperature). Then : $T_{int\ liq\text{-}sol}=T_{MG}$

This solid has the composition $C_s(T_{MG})$ *at the interface*. According to the considered phase diagram, this solid is the same at the interfaces with both liquid layers L1 and L2. But a difficulty appears here: unlike the case analysed for standard non-eutectic mixtures, the liquid, at the interface, which is in equilibrium with the solid, has not the composition C_{L1} or C_{L2} of the considered liquid layers, but should have the composition C_1 (with $C_1<C_{L1}<C_{L2}$) or C2 . The consequence is that both liquids may undergo a separation (formation of liquid globules) in the temperature gradients (mainly boundary layers). The effect of this separation on heat transfer is not known. Nevertheless, for reactor materials, the reciprocal solubility of both liquids is limited. Thus, the expected relative amount of separated liquid in the boundary layer is small and should have only a small effect on the heat transfer.

This case will be analysed separately below (§ 2-2 and 2-3) and the relative amount of separated liquid will be determined.

The thermalhydraulic constraints

Mass conservation and thermalhydraulic constraints permit to close the system of equations.
Heat transfer considerations provide links between power dissipation, temperatures and heat flux distributions between the two layers and between the layers and the solid interface.

Thus, a second link between the interface temperature $T_{int\ L1,L2}$ and the heights of the liquid layers is provided by heat transfer considerations.

The liquid/liquid interface may simply be considered, from the point of view of heat transfer, as a rigid interface having temperature $T_{int\ L1,L2}$.

The choice of the heat transfer correlations must be performed adequately according to the characteristics of the heat transfer between layers (stable or unstable stratification) which depends on the repartition of the heat sources, and accordingly, to the size of the pool (laminar or turbulent boundary layers). When the power is dissipated in the liquid situated at the bottom, the presence of the top layer (with absence of crust at the interface between both liquids) acts as an additional heat transfer resistance towards the top surface. The consequence is that the power transmitted to the top surface decreases in comparison to the case of a homogeneous pool.

Status of model validation

General approach

For the moment, the SIMECO experiments are the only analytic experiments we know on corium pool simulation with the presence of a miscibility gap. We will use these results to validate directly or indirectly following aspects of the model :

- The interface condition between the two liquid phases ($Tint_{L1,L2}$) and the relative amount of the two layers (§ 2.1),
- The effect of the 2 liquids separation in a temperature gradient when $T_{int\ L1,L2} < T_{max,\ MG}(C_0)$ (§2.3)
- The return to a single liquid behaviour when $T_{int\ L1,L2} > T_{max,\ MG}(C_0)$ (§ 2.2)

The interface condition between liquid L1 and the solid ($Int_{L1,\ solid}$) and the interface condition between liquid L2 and the solid ($Int_{L2,\ solid}$) cannot be validated on the basis of these experiments since SIMECO MG experiments do not include a solid phase at the boundaries. Some specific experiments would be necessary.

The SIMECO MG experiments

The SIMECO experiments have been performed by RIT [Theerthan et al., 2000]. The test section (figure 4a) represents a 2D slice hemisphere of a lower head at small scale (diameter is ~ 50 cm). A submerged resistor is used for heating the fluid, in the BBO layer (simulation of residual power). The fluid used is a mixture of Benzyl Benzoate(BBO) and of Paraffin oil (PO). PO is lighter than BBO. This mixture undergoes a separation in the liquid phase according to the phase diagram given by the authors and reproduced in figure 4b.

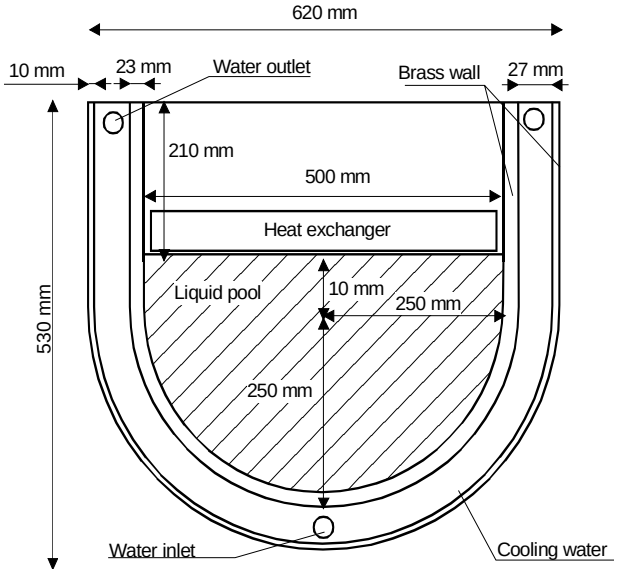

Figure 4a : Sketch of the SIMECO test device [Theerthan et al., 2000]

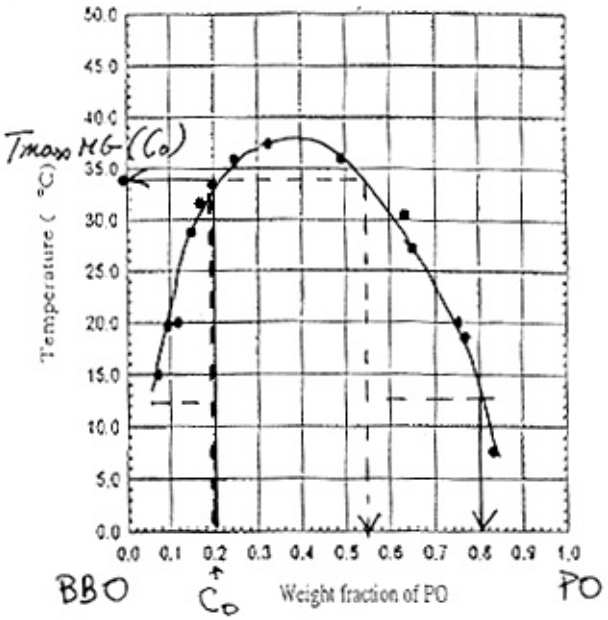

Figure 4b: Miscibility gap in the liquid BBO - liquid PO system used for SIMECO tests [Theerthan et al., 2000-1].

As the boundary (top and bottom) was cooled by means of a flow of water at a temperature of ~ 12 °C (285 K), the mixture did not freeze on the boundaries ($T_{boundary}>T_{MG}$). No solid phase is present on the boundaries. Therefore the boundary condition is imposed, here, by the external cooling and by the heat transfer through the walls plus heat exchange with the coolant. The authors have performed transient experiments, starting from a cold liquid mixture (26 cm BBO and 4 cm PO; i.e. ~20 w% PO). The power was switched on and the temperature variations in the mixture as well as the power distribution were followed during the heat-up transient. The minimum power level dissipated in the fluid during the experimental programme was approximately 600 Watts

Validation of the model at the interface between the two liquid phases (Int $_{L1,L2}$) and for the existence of two layers

Some parametric calculations have been performed on the basis of the model described above, and only for steady state situations (from the point of view of thermalhydraulics and physicochemistry (mass transfer)). There are some uncertainties affecting the heat transfer at small scales. Therefore, different correlations will be considered for the heat transfer:

a) Lower, heated pool; heat transfer to the bottom curved surface:

[Mayinger et al., 1976] : $Nu_{l,b} = 0.55\,Ra_i^{0.2}$

[Kelkar and Patankar, 1993]: $Nu_{l,b} = 0.1\,Ra_i^{0.25}$

b) Lower, heated pool; Heat transfer to the top (Interface with the upper layer)

[Mayinger et al., 1976] : $Nu_{l,top} = 0.4\,Ra_i^{0.2}$

[Kelkar and Patankar, 1993]: $Nu_{l,top} = 0.18\,Ra_i^{0.237}$

c) Heat transfer at the upper and lower surface of the upper layer:

The heat transfer is governed by Rayleigh Bénard (RB) instabilities on both upper and lower horizontal surfaces of the upper layer. Following heat transfer correlation is used [Bernaz et al., 2001]:

$$Nu_{RB} = 0.14 Ra^{\frac{1}{3}}$$

d) Heat transfer on the lateral surface of the upper layer:

The thickness of the upper layer is small (<4cm), therefore the heat transfer on the lateral surface is considered to be controlled by laminar boundary layer flow ($Gr<10^9$). To describe this heat transfer, the [Churchill & Chu, 1975] correlation for laminar boundary layer flow is considered:

$$Nu_{up,lat} = 0.508 \,\mathrm{Pr}^{\frac{1}{4}} \left(\frac{20}{21} + \mathrm{Pr}\right)^{-\frac{1}{4}} Ra^{\frac{1}{4}}$$

with

$$Ra_i = \frac{g\beta q H^5}{\lambda \nu \alpha}$$

$$Ra = \frac{g\beta \Delta T H^3}{\lambda \nu \alpha}$$

$$Nu = \frac{hL}{\lambda}$$

L: characteristic dimension of the considered layer (m)

g: gravity acceleration (m/s²)

Pr: Prandtl number of the fluid layer

H: height of the layer (or pool) (m)

Q: volumetric heat dissipation (W/m^3)

ΔT : temperature difference between maximum temperature in the layer (pool) and boundary temperature (K)

β : volumetric expansion coefficient (K^{-1})

λ : thermal conductivity of fluid in considered layer (W/mK)

ν : kinetic viscosity of fluid in considered layer (m²/s)

α : thermal diffusivity of fluid in considered layer (m²/s)

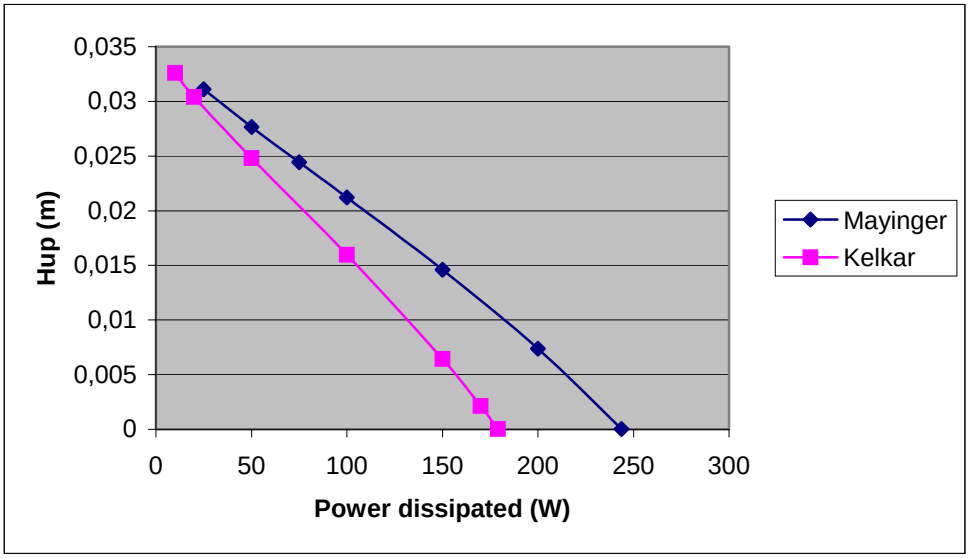

Figure 5: Variation of the height of upper layer vs. Power calculated in the SIMECO MG configuration

Figure 5 shows the calculated evolution of the height of the upper layer (L2) as a function of the power, in thermalhydraulic steady state. The two curves correspond to the results obtained with the two sets of heat transfer correlations. The height of this layer (L2) decreases when the power increases and its composition tends from PO containing 20 % BBO at 12°C (285 K) to PO containing 45 % BBO at 34 °C (307 K). This temperature corresponds to $T_{max,MG}(C_0)$, considering the initial amounts of the species (PO and BBO) in the mixture. According to the calculations, the top layer disappears for power levels greater than, approximately, 250 W. This is in accordance to the conclusion of the authors who state that, for power levels equal or higher than 600 Watts (minimum experimental power level), the top layer dissolves completely into the bottom fluid during the heat-up transient. This rather low power threshold is linked to the low temperatures of existence of the miscibility gap for the considered PO + BBO mixture ($T_{max,MG}(C_0)$ ~34°C) and to the low thermal conductivity of the considered products. Such a complete dissolution would not be possible in a reactor case, due to the limited reciprocal solubility of metallic and oxidic phases in the temperature range of interest ($T_{max,MG}(C_0)$ is much higher than the temperature range of interest). In the reactor situation, a steady state regime with two liquid layers at physicochemical equilibrium can be obtained (discussion in part 3).

The calculated evolution of the power partition $\frac{W_{top}}{W_{bottom}}$ versus the total Power dissipation is given on figure 6, for the cases where the liquid L2 exists. For single liquid pools, this power ratio tends towards unity [CSNI, 1998]. W_{top} is the power evacuated through the upper, horizontal, surface and W_{bottom} is the power evacuated through the bottom, curved, surface.

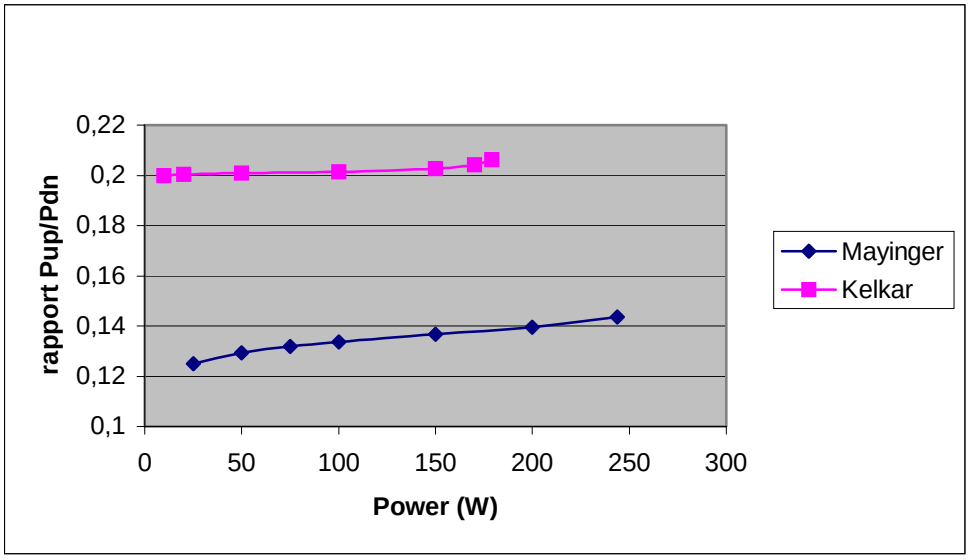

Figure 6: Calculated variation of $\frac{W_{top}}{W_{bottom}}$ vs. Power in SIMECO, limited to the power range for which two liquid layers exist.

The calculated power ratio $\frac{W_{top}}{W_{bottom}}$ ranges from approximately 12% to 20%. The authors [Theerthan et al., 2000-1] indicate that this power ratio is characteristic for two non-miscible layered liquids [Theerthan et al., 2000-2] and varies between 27% and 37% during the two layer existence period for the experiments performed with PO and BBO. However, no steady state situation with two layers has been obtained for the latter experiments since the minimum power level was 600 Watt. The latter results are derived from transient measurements performed during the transient heat-up period corresponding to the dissolution process of the top layer (during this process two layers exist).

Pool behaviour after dissolution of the top layer

The top layer disappears and the pool comes to a single liquid when $T_{int\,L1,L2} > T_{max,MG}(C_0)$. The pool behaves globally like a single liquid with T_{MG} as interface temperature with the solid boundary. The single liquid behaviour corresponds to the observations of the experimentalists [Theerthan et al., 2000-1]. However, in this case also, the liquid does not exactly behave as a single liquid since it undergoes, according to preceding considerations, a separation in the temperature gradients, mainly in the boundary layers (see figure 7). In this case the centre of the pool (where $T > T_{max,MG}(C_0)$) is homogeneous and liquid phase separation occurs in the boundary layers (where $T < T_{max,MG}(C_0)$). The experimentalists confirm that a separation occurs in the boundary layer [Theerthan, 2001], but do not provide more detailed information about size of droplets, composition and relative movements of the separated fluid (due to different density).

In this case, the whole spectrum of liquid compositions between C1 and C_0 and between C'_0 and C2 can, theoretically, be obtained in the boundary layers. The composition of the carrying (major) liquid will depend on the average composition C0 (L1 in the case considered here).

N.B.: C'_0 is the composition of liquid L2 at $T_{max,\,MG}(C_0)$

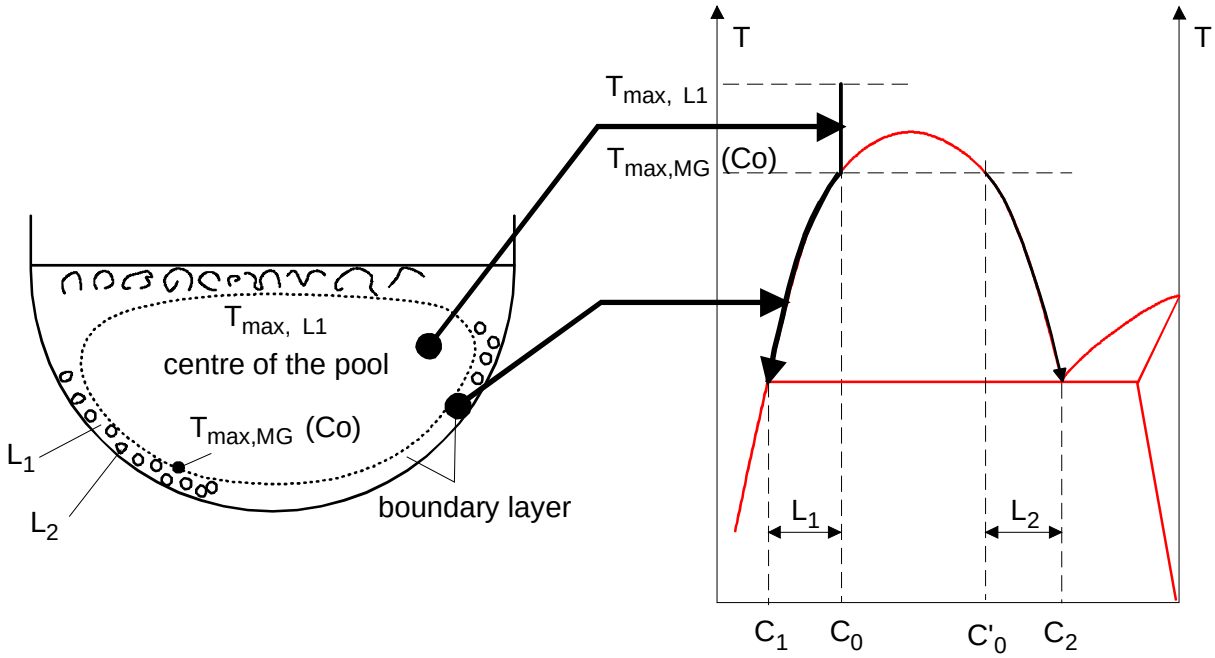

Figure 7 "Single" liquid behaviour and liquid-liquid separation at the boundaries when: $T_{int\,L1,L2} > T_{max,\,MG}(C_0)$

Two liquid separation in the boundary layer when $T_{int\,L1,L2} < T_{max,\,MG}(C_0)$.

This effect is directly linked to the non-uniform temperature distribution in the layers. Where $T > T_{int\,L1,L2}$, the liquid is homogeneous. This is generally the case for the inner part of the liquid L1. In this case the power is mainly dissipated in this liquid (L1) and the maximum temperature in this liquid (Tmax, L1) is higher than the interface temperature $T_{int\,L1,L2}$. Figure 8 shows the corresponding area of the pool and the connection to the phase diagram.

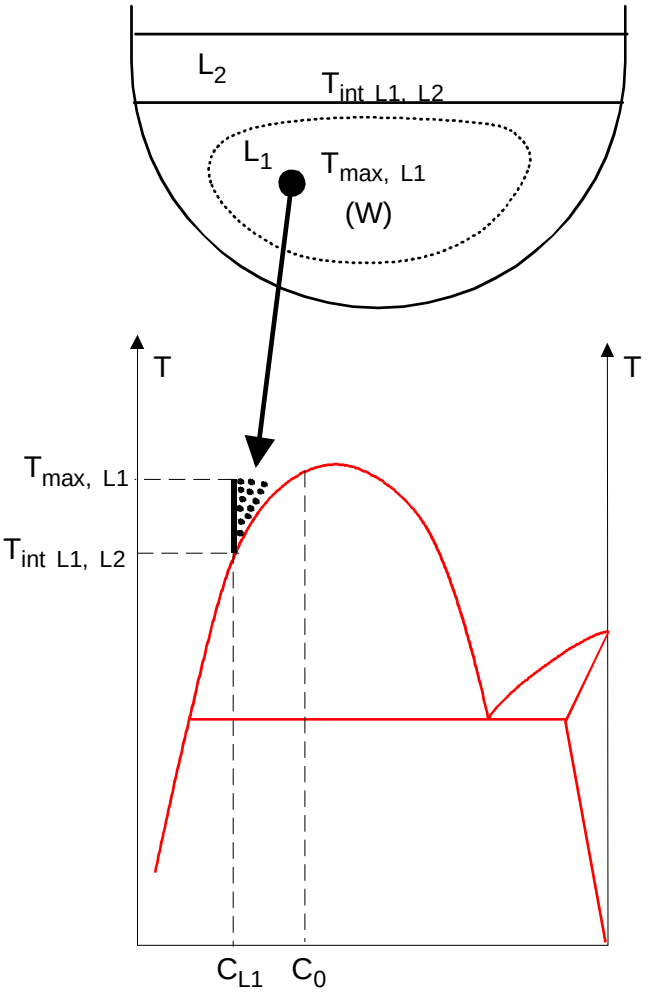

Figure 8: Hot zone in L1 and Corresponding area on phase diagram (where T> $T_{int\ L1,L2}$) ; case: $T_{int\ L1,L2} < T_{max,\ MG}(C_0)$

Where $T < T_{int\ L1,L2}$ the compositions of both liquids follow the curves L1 and L2. This means that liquid L1 tends towards the composition C1, and, thus, that some non-miscible liquid L2 appears, with minor amounts, within the liquid L1 (see figure 9). The maximum amount of liquid L2 in liquid L1 is obtained at the cold boundary where $T=T_{MG}$, this amount is given by:

$$x_{L2\ in\ L1}(T_{MG}) = \frac{C_{L1} - C_1}{C_2 - C_1}$$

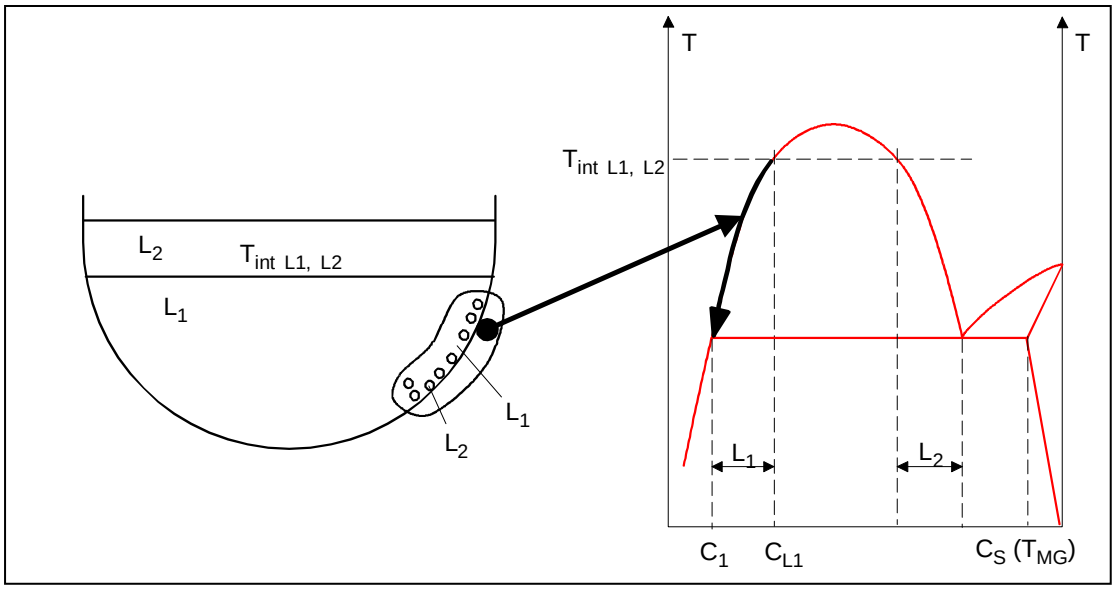

Figure 9: Boundary layer in L1 and corresponding area on the phase diagram (where T< $T_{int\ L1,L2}$); case: $T_{int\ L1,L2} < T_{max,\ MG}(C_0)$

Correspondingly, the composition of liquid L2 tends towards the composition C2 and some minor liquid L1 appears within L2 with a maximum amount given by:

$$x_{L1\ in\ L2}(T_{MG}) = \frac{C_2 - C_{L2}}{C_2 - C_1}.$$

Now, from the hydrodynamic point of view, if the minor liquid is supposed to be entrained and to follow the flow of the major (carrying) liquid, these liquids will recombine into a single liquid at higher temperature in the vicinity of the central hot part of the pool. Supposing that, due to the different densities, the minor liquid tends to separate from the major liquid leads to more complex situations. These situations may perhaps lead to instabilities which are not investigated in the present development.

Time delay necessary to reach thermalhydraulic steady state and physicochemical equilibrium between layers

In the reactor case, the time delay necessary to reach steady state (established heat flux distribution) is mainly controlled by scenario aspects (corium relocation path between core and lower head, debris remelting, etc…). It is not the aim here to deal with all these complex problems. The aim is to provide and compare characteristic time delays which are necessary to reach thermalhydraulic steady state and physicochemical equilibrium starting from a given, simplified, initial condition. The objective is to conclude if physicochemical equilibrium may be reached in the reactor case.

The initial condition which will be considered here is a hemispheric geometry with a layered molten corium at the melting temperature of the oxidic phase ($T_{liquidus\ oxide}$). The thermalhydraulic time delay is estimated by supposing that the heat up transient in the fluid is controlled by natural convection [Seiler, 1988].

$$\tau_{convection} \sim \frac{\rho R C_p}{h}$$

The characteristic time delay to reach physicochemical equilibrium is derived by supposing that the mass transfer between layers is limited by diffusion in a mass transfer sublayer (δ). This time delay is maximized by considering thick corium layers (*H*). In reality, the mass transfer takes places during the remelting process and the delay is shorter than the time delay estimated here. The mass transfer is mainly controlled by the oxidic phase and the characteristic delay time for reaching physicochemical equilibrium is given by [Defoort, 2002]:

$$\tau_{physicochemical} = \frac{\delta H}{D}$$

where:

δ is the thickness of the mass transfer sublayer, in the oxidic phase (m)

H is the thickness of the oxidic layer (m)

D is the molecular diffusivity in the oxidic liquid (m²/s)

ρ is the density of corium (kg/m^3)

C_p is the specific heat of corium (J/kg K)

R is the radius of the hemisphere (m)

h is the average heat exchange coefficient (W/m² K)

The thickness of the mass transfer sublayer is linked to the convection (thermalhydraulics). If natural convection is dominant this thickness is given by:

$$\frac{\delta}{H} = (GrSc)^{-\frac{1}{3}}$$

where

Gr is the Grashof number characterizing the convection in the layer

Sc is the Schmidt number ($Sc = \frac{\nu}{D}$)

ν is the kinematic viscosity (m²/s)

The diffusion coefficient is estimated with the Stokes-Einstein equation (see appendix A). Its validity for corium mixtures is highly questionable. The uncertainty affecting the molecular diffusivity is estimated to a factor ~10^2 for In-Vessel corium (D ranges between 10^{-7} and 10^{-9} m²/s) inducing an uncertainty on the time necessary to reach physicochemical equilibrium of a factor ~20.

Applying preceding relations for In-Vessel corium (H~1 metre; Gr~10^{15}), following characteristic time scales are obtained:

$\tau_{convection}$ is of the order of one (1) hour

$\tau_{physicochemical}$ varies between approximately a few minutes and one hour depending on the assumption on the mass diffusion coefficient.

It can thus be concluded that, despite the poor knowledge of the mass diffusion coefficient, thermalhydraulic steady state and physicochemical equilibrium can be obtained practically within the same time delay for In-Vessel situations.

Separation in the boundary layers

Some specificity linked to real corium mixtures tend to moderate the preceding considerations: generally $T_{max,MG}$ is very high for corium (boiling is the real limitation for reactor pressure range) and, as a consequence, the curves L1 and L2 are very steep near to the edges of the miscibility gap (C1 and C2) and the maximum temperature which can be reached in the reactor is lower than $T_{max,MG}$ and even lower than the boiling temperature. This means that $C_2 - C_{L2} << C_2 - C_1$ and that $C_{L1} - C_1 << C_2 - C_1$: the variation of composition of both liquids L1 and L2 (due to the decrease of the temperature in the boundary layers) should then be small.

Also, when the temperature $T_{int\ L1,L2}$ approaches $T_{max,MG}(C_0)$, the global amount of liquid L2 is reduced ; the pool is mainly formed of liquid L1 whose composition is close to the average composition of the mixture: C_0.

Reactor application

An evaluation has been made of the mass of steel which can lead to density inversion when coming in physicochemical equilibrium with the oxidic phase. Density inversion means that the density of the metallic phase becomes greater than the density of the oxidic phase. This density increase is due to dissolution of uranium into the metallic phase. For the reactor application a bounding situation is considered. This bounding situation is sketched on figure 10 and is based on following main hypotheses:

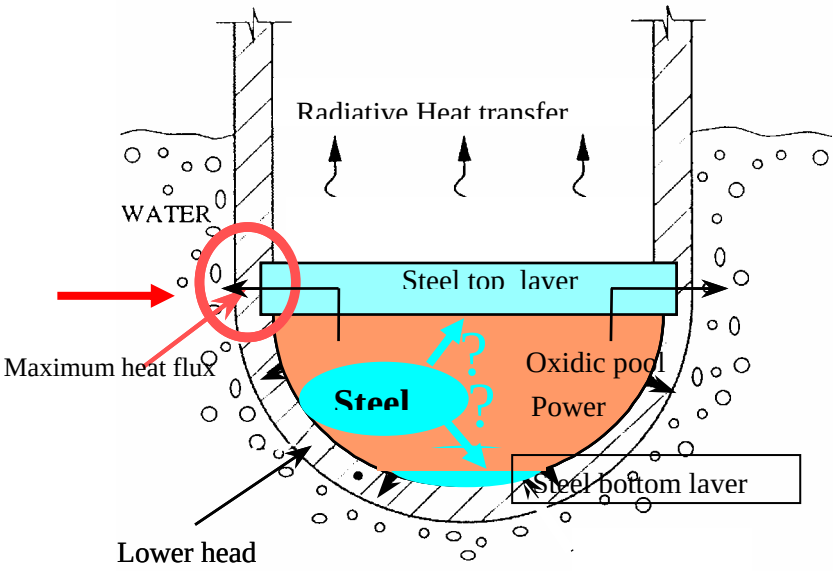

Figure 10: sketch of reactor situation

- Steel reacts with U-Zr-O mixture and forms a bottom metal layer,
- The mass of steel that is contained in the bottom layer (M_{SSbot}) corresponds to the maximum mass of steel that can stratify below the molten oxide layer. The steel contained in the bottom metal layer is in thermodynamic equilibrium with the molten oxide layer (no crust at the interface),
- Additional molten steel stratifies on top of the molten oxide layer. This top steel layer does not come to physicochemical equilibrium with the oxide layer. An oxidic crust separates the oxidic layer from the top steel layer,
- There is no Zr is the top steel layer
- Heat is transferred from the surface of the top steel layer to upper reactor structures by radiation only. The temperature of the structures is taken at melting temperature of steel (i.e.~ 1500°C). Two cases are considered for the emissivity of molten steel: 0,15 (liquid steel under inert atmosphere) and 0.45 (liquid steel under oxidizing atmosphere).
- The minimum mass of steel that is necessary for keeping the heat flux to the vessel below CHF (focusing effect) in the top layer (M_{SStop}) is calculated
- The CHF is taken at 1,5 MW/m²
- The total mass of steel that is necessary to keep the heat flux below CHF is calculated as: $M_{SStot} = M_{SSbot} + M_{SStop}$

The calculations are conducted for two application cases:

- Case 1: UO2: 75 tonnes, U/Zr = 1,2 vessel diameter: ~3,5 m
- Case 2: UO2: 100 tonnes, U/Zr= 1,45 vessel diameter ~4 m

The degree of oxidation of zirconium has also been varied between 0% (C0) and 50 % (C50). Below the denomination Cox will be used; ‘ox’ designates the percentage of oxidized zirconium.

The calculation results concerning M_{ssbot}, the maximum mass of stainless that can stratify below the oxidic melt is given on table 1. The figures given is the table are average values taken from IRSN and CEA calculations results that are compatible with MASCA tests results. [Barrachin, Defoort, 2004].

	U/Zr = 1,2	U/Zr = 1,45
	75 t UO2	100 t UO2
C0	~ 49	~ 50
C10		~ 45
C20		~ 30
C25	~ 26	~ 28
C30	~ 22	~ 22
C40	~ 15	~ 13
C50	~ 7	

Table 1: Calculated maximum mass of steel (in tonnes) that is expected to stratify below the oxidic layer. The uncertainties are nor reported here (see the paper from Barrachin and Deffort) but are still large.

The resulting total mass of steel that is required for keeping the heat flux below the CHF is given on table 2 for case 1 and on table 3 for case 2.

	Surface emissivity of molten steel = 0,15				Surface emissivity of molten steel = 0,45			
	Hmin (cm)	**$M_{SS\ top}$ (t)**	**$M_{SS\ bot}$ (t)**	**$M_{SS\ tot}$ (t)**	**Hmin (cm)**	**$M_{SS\ top}$ (t)**	**$M_{SS\ bot}$ (t)**	**$M_{SS\ tot}$ (t)**
C25	45	35	26	**61**	25	19	26	**45**
C30	45	35	22	**57**	25	19	22	**41**
C40	45	35	15	**50**	25	19	15	**34**

Table 2: Bounding approach for case 1: bottom and top stratification. Minimum mass of steel necessary for keeping the heat flux below CHF (U/Zr = 1,2 and 75 tonnes UO2)

	Surface emissivity of molten steel = 0,15				Surface emissivity of molten steel = 0,45			
	Hmin (cm)	**$M_{SS\ top}$ (t)**	**$M_{SS\ bot}$ (t)**	**$M_{SS\ tot}$ (t)**	**Hmin (cm)**	**$M_{SS\ top}$ (t)**	**$M_{SS\ bot}$ (t)**	**$M_{SS\ tot}$ (t)**
C25	66	66	28	**94**	53	53	28	**81**
C30	66	66	22	**88**	53	53	22	**75**
C40	66	66	13	**79**	53	53	13	**66**

Table 3: Bounding approach for case 2: bottom and top stratification. Minimum mass of steel necessary for keeping the heat flux below CHF (U/Zr = 1,45 and 100 tonnes UO2)

From these calculations it can be observed that the mass of steel that is calculated to stratify below the oxidic layer is significant, even the case where 40% of the zirconium is oxidized. The metal layer that relocates under the oxidic pool has practically no impact on the fraction of residual power that is transmitted to the top steel layer. Thus, it has practically no impact on the minimum thickness of the top steel layer that is necessary for keeping the heat flux below CHF. This results in a significant increase of the total mass of steel that is necessary for keeping the heat flux below CHF.

Conclusions

A model is proposed describing the corium pool behaviour with a material composition presenting a miscibility gap (MG). The model is described in the first part of this paper and the state of its validation is developed in the second part, against SIMECO experiments. Qualitatively the model predicts the experimental behaviour (domain of existence of two layers, phase separation in the boundary layers and power split).

Applicability to reactor situation is discussed. It is also concluded that the time delay to obtain physicochemical equilibrium between liquid phases is of the same order of magnitude than the time delay necessary to obtain thermalhydraulic steady state (established heat flux distribution). Melt configurations involving contact between liquid oxide and liquid metal can be obtained. Order of magnitude of steel mass which can lead to density inversion (metallic phase heavier than oxidic phase) are estimated. A significant mass of steel can relocate in the bottom layer (10 to 20 tonnes for 40% zirconium oxidation). This increases significantly the total mass of steel that is necessary for keeping the heat flux below CHF.

Further R&D needs

The main uncertainties are linked to the U-O-Zr-SS thermochemical melt behaviour and to the calculation of the densities of the layers. Research priorities should be attributed to the elaboration of thermodynamic data bases and to the methodology of liquid mixtures density calculation.

References

Asmolov V., 2001 "MASCA project workscope" 2nd MASCA PRG Meeting Finland Helsinki April 17-18, 2001

Barrachin M., Defoort F. 2004, MASCA programme contribution to the material aspects of In-Vessel Corium OECD MASCA Seminar June 10-11 Aix en Provence, France

Bechta S., 2001 "Zr partitioning tests in the cold crucible test MA-1" OECD MASCA meeting, April 17-19, Helsinki

Bernaz L., Bonnet J.M., Seiler J.M., 2001 “Investigation of natural convection heat transfer to the cooled top boundary of a heated pool” Nuclear Engineering and Design n°204, 2001, pp 413-427.

Bonnet J.M., Seiler J.M., 2001 "In-Vessel Corium Pool Thermalhydraulics for the Bounding Case" OECD RASPLAV Project. Note SETEX/LETM 01-247

CSNI, 1998 "In-Vessel Core Debris Retention and Coolability" Workshop Proceedings 3-6 March 1998 Garching near Munich, Germany

Churchill S.W. & Chu H.S. “Correlating Equations for laminar and turbulent free convection from vertical plate” Int. J. Heat and Mass Transfer, 1975, Vol. 18 pp 1323-1329

Defoort F., 2002 Internal CEA report SETEX 02-286

Gueneau C., Dauvois V., Perodeaud P., Gonella C., Dugne O., 1998 "Liquid immiscibility in a (U,O,Zr) model corium" Journal of Nuclear Materials, n°254, pp 158-174

Gueneau C., 1999 CEA note DPE/SPCP/NT-99-042

Gueneau C., 2003 to be published in Journal of Nuclear Materials in 2003

Hayward P.J., George I.M., “Dissolution of UO2 in molten zircalloy 4” Journal of Nuclear materials, 232, 1996

Hofmann P., 1976 „Reactions- und Schmelzverhalten der LWR-Corekomponenten UO2, Zircaloy and Stahl wärhend des Abschmelzperiode“ FKF 2220, Juli 1976

Kelkar K.M., Patankar S.V., 1993 "Turbulence model for melt pool natural convection heat transfer" ANS Reactor Safety meeting Oct 25-28 1993 Washington D.C.

Kim K.T., Olander D.R., 1988 „Dissolution of Uranium Dioxyde by Molten Zircaloy“ Journal of Nuclear materials, 154, 1988, pp 85-101

Mayinger F., Jahn M., Reineke H.H., Steinberner U., 1976 "Examination of thermohydraulic processes and heat transfer in a core melt" BMFT RS 48/1 Hanover, Germany

Parker G.W., 1982 Proc. 10th water Reactor Safety Rea=search Information Meeting, Nureg/CP-0041, vol 2, Gaithersburg, MD, October 1982.

Parker G.W., Hodge S.A., 1990 “Small scale BWR Core Debris Eutectics Formation and Melting Experiment” Nuclear engineering and Design, 121, 1990, pp 341-347

Powers D.A., 1987 “Chemical phenomena and FP behaviour during Core Debris/Concrete Interactions” Proc. CSNI Specialist Meeting on Core Debris Concrete Interaction EPRI NP-5054-SR February, 1987

RASPLAV Seminar GRS Munich, Germany 14-15 November 2000

Rempe J.L., Knudson D.L., Allison C.M., Thinnes G.L., Atwood C.L., Cebull M.J., 1997 "Potential for AP600 In-Vessel Retention through Ex-Vessel Flooding" INEEL/EXT-97-00779

Seiler J.M., 1988 “Cooling of molten material liquid pool submitted to volumetric heating” International ENS/ANS conference on thermal reactor safety. 2-7 October 1988 Palais des Papes Avignon.

Seiler J.M., Froment K., 2000 "Material effects in late phases of severe accidents" Multiphase Science and Technology Vol 12 pp 117-257 issue 2000

Theerthan S.A., Kolb G., Sehgal B.R. , 2000-1 "The role of phase separation on heat transfer in internally heated liquid layers" Proc. ICONE 8th International Conference on Nuclear Engineering April 2-6, 2000, Baltimore USA

Theerthan S.A., Kolb G., Sehgal B.R., 2000 “Heat transfer in internally heated liquid layers with stable stratification induced by phase separation” Proc. of Nat. Heat Transfer Conf., Pittsburg, PA, USA, 20-22 August 2000

Theerthan S.A., 2001 Personal communication. ARVI Meeting, Paris, July

Appendix A

Stokes-Einstein equation:

$$D = \frac{k_{Bol} T}{\alpha \pi \mu F}$$

$$4 \le \alpha \le 6$$

$$F = \left(\frac{\mathrm{M}}{\varepsilon} \frac{3}{4\pi\rho \, \mathrm{N}_a} \right)^{1/3}$$

F	is the molecular radius of diffusing species (m)
T	is the temperature (K)
k_{Bol}	is the Boltzmann constant (1,3806 10^{-23} J/K)
M	is the molar weight of the fluid (kg/mol)
ε	is the volumetric packing fraction
μ	is the dynamic viscosity of the fluid (kg/ms)
ρ	is the density of the fluid (kg/m^3)
N_a	is the Avogadro number (mol^{-1})